

Defect-mediated half-metal behavior in zigzag graphene nanoribbonsR. Y. Oeiras,¹ F. M. Araújo-Moreira,¹ and E. Z. da Silva²¹*Department of Physics, Federal University of São Carlos, 13565-905 São Carlos, SP, Brazil*²*Institute of Physics “Gleb Wataghin,” University of Campinas-Unicamp, 13083-970 Campinas, SP, Brazil*

(Received 22 April 2009; published 18 August 2009)

In this work, we present *ab initio* studies of the electronic and transport properties of carbon nanoribbons with structural defects: divacancies and divacancies combined with the Stone-Wales-like (SW) defects. Simulations with defects in different positions with respect to the ribbons indicated that the total energy of the ribbon is lower when the defect is at the ribbon edge. This indicates that the relation defect edge is of fundamental importance to find the minimal energy configuration. All ribbons studied in this Brief Report show a high spin polarization in the transmittance, in some cases more than 90%, showing an almost half metal behavior suggesting them as possible candidates to be used as spin filter systems.

DOI: [10.1103/PhysRevB.80.073405](https://doi.org/10.1103/PhysRevB.80.073405)

PACS number(s): 73.63.-b, 72.25.-b, 72.80.Rj, 73.22.-f

Graphenes are the building blocks for many structures, from the old graphite to the modern produced fullerenes¹ and carbon nanotubes.² In the recent years, it has become an important structure since experimental synthesis of stable single graphene layer at room temperature was achieved.³⁻⁶ Besides being an interesting structure due to its the unusual massless Dirac Fermion behavior,⁷⁻⁹ it shows promising possibilities as a material to be used for devices due to its high conductivity and almost perfect structure. Graphenes can be also be used as building blocks of new quasi-one-dimensional structures called graphene carbon nanoribbons (GCNR). These new structures, consisting of very small stripes, can have different types of edges. The most important are the armchair and the zigzag edges, respectively. The experimental analysis of these edges with scanning tunneling microscopy suggested the presence of a large amount of electronic edge states at Fermi level.^{10,11} These results have also been confirmed by theoretical studies.¹²⁻¹⁵

In the case of nanoribbons with zigzag edges (we call ZGNR), studies suggested that the edge atoms exhibit a liquid magnetic moment.¹⁶ The ZGNR ground state presents a semiconducting behavior and each zigzag edge has ferromagnetic ordering with antiparallel spin orientation between the two edges. There are several studies about the electronic and structural properties of graphene and carbon nanotubes with structural defects. Divacancy is a type of defect produced by removing two neighboring atoms. The study of those structures formed by vacancy-like defects in graphene suggested that the vacancy and divacancy have nearly the same formation energy if the chemical potential is close to the value for graphene,¹⁷ indicating that the divacancy is a more stable defect. Recently, it has been reported a work¹⁸ where, by tight-binding molecular dynamics, authors have shown that spatially separated vacancies in a graphene sheet can coalesce to form divacancies. These defects were studied in carbon nanotubes and graphene systems, where changes in the transport and electronic properties were discussed.¹⁹

In the present work, we considered the effect of defects in the electronic, structural and transport properties of ZGNR. A study of ZGNRs doped by Boron (a donor impurity), indicated that perturbations in π/π^* states affected strongly their transport properties²⁰ producing an anisotropy between the up and down channels. This striking result indicates that,

in future, ZGNRs could be used in novel area of spintronics, specifically as spin filter. Defects introduce stronger perturbations than impurities on electronic states of ribbons and can induce larger spin polarization, motivating the study of transport properties of these systems. One important point that emerged from our transport studies in ZGNR with defects was the strong spin dependence of the transport channels where we observed the departure from the spin degenerate result of $0.5G_0$, per spin channel (where $G_0=2e^2/h$ is the quantum of conductance), for the perfect ZGNR, to situations close to half metal behavior in some of the structures studied.

Our structural studies were made using the SIESTA code²¹ that is based in the framework of density functional theory (DFT).²² For electronic and structural relaxation of atomic positions, we used: Troullier-Martins pseudopotential²³ with generalized gradient approximation (GGA) of Perdew-Burke-Enzerhof,²⁴ a double- ζ polarization basis (DZP) for all ribbon atoms and a mesh cutoff of 300 Ry for the integration grid in real space. All atoms were relaxed until the forces were smaller than $0.02 \text{ eV}/\text{\AA}$. The transport properties of ZGNR were studied with the TRANSAMPA code²⁵ that is based in framework of the nonequilibrium green functions²⁶ and DFT. We considered GNRs (5,0)²⁰ with a scattering region with 126 atoms for the pure ribbon and 124 atoms for ribbons with divacancies. The leads were similar to the ones used previously in Ref. 20 also (5,0) GNRs with 56 atoms for each lead. The transmittance shape can be understood by an analysis of the spatial distribution of the electronic states,²⁷ for this reason, we also studied the local density of states (LDOS) at Fermi level using the green function from the transport calculation.

We labeled the studied defects as follows: 585, defect formed by two pentagons and one octagon, 555777 formed by three pentagons and three heptagons, and 5557777, four pentagons and four heptagons. The total energies of the ZGNRs vary with the defect position in the ribbons. Figure 1 shows all the structures simulated in this work. All energies were referred to the value of structure (a). Nanoribbons displayed in (a), (b), and (g) showed just the divacancy defect (585) while ribbons (b), (c), (d), and (f) displayed divacancies combined with SW defects forming 555777 and 5557777 defects. In the case of a graphene sheet, an *ab*

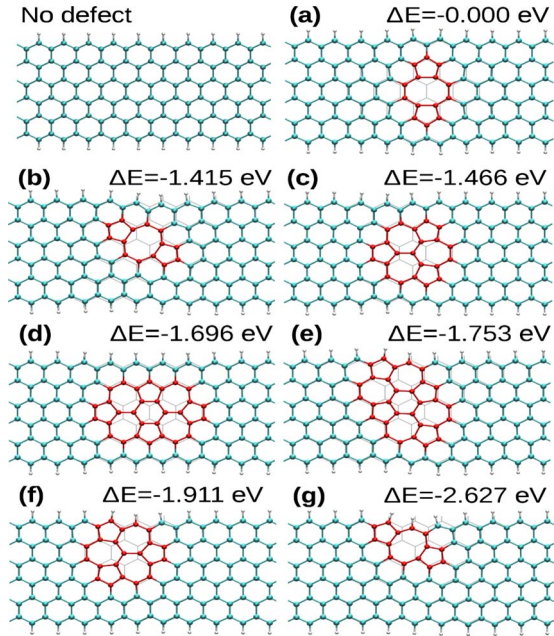


FIG. 1. (Color online) The ZGNRs with defects and with energies referred to structure (a) ($\Delta E = E_{(x)} - E_{(a)}$, where x refer (b)–(g) cases). (a) 585 defect at the center, (b) 585 defect rotated near center, (c) 555777 defect at the center, (d) 5557777 defect at the center, (e) 5557777 defect rotated from center toward the edge, (f) 555777 defect at the edge, and (g) 585 defect at the edge.

initio study¹⁴ of defects indicated that the 555777 is more stable than the 585 one by a value of 0.9 eV. A similar study with carbon nanotubes indicated the opposite behavior, namely the 585 being more stable than the 555777 structure due to the tube curvature.¹⁵

The energies of the ribbons with 555777 and 5557777 defects were smaller than the energies of the 585 ribbons, when the defects were at the center of the ribbon, in agreement with the behavior in graphene. On the other hand, if the defects were near the edge, the 585 defect became more stable than the 555777 one. An explanation for this behavior can be found in the bond length of the carbon atoms. If the pentagon bonds were near the average bond length, as in the perfect ribbon, the chemical bond would be better formed, providing the smallest total energy. In the ribbons (a) and (b), we noticed two bond lengths (between 1.55 and 1.67 Å, respectively) larger than the average value for bonds in these ribbons (between 1.42 and 1.46 Å). These two bonds were in the pentagons of the defect. In the (g) case, we observed that two bonds had 1.54 Å length, showing a better formation of pentagon bonds than the other cases with the 585 defect, justifying the decrease in the total energy in this case.

The structure depicted in Fig. 1(b) presented an overall larger deformation and also larger pentagon bonds than ribbon (g), suggesting that this as the reason for the larger energy for ribbon (b) by 1.2 eV. To confirm this idea, we simulated these two ribbons with this defect but without allowing the atoms to relax into new configurations and then calculated the total energy. The energy difference between the two ribbons was 197 meV, indicating that the contribution of the edge to the total energy is small. Therefore, the energy dif-

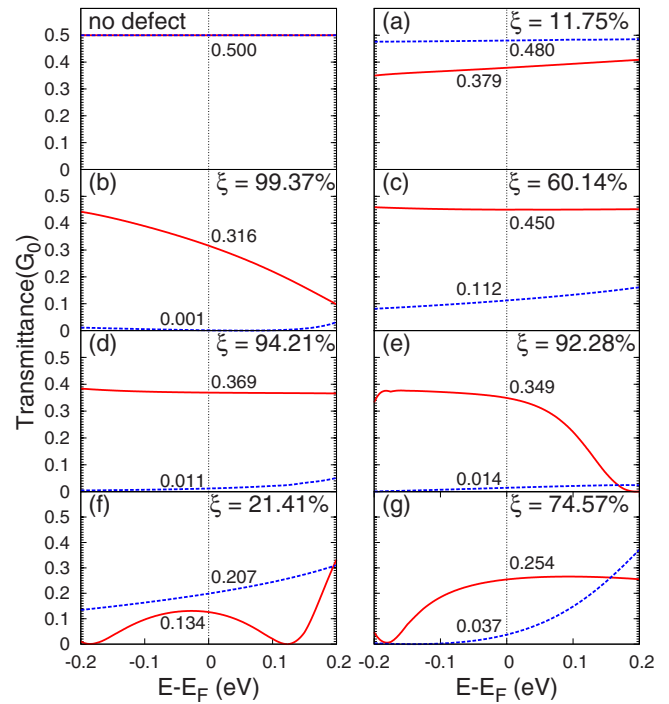


FIG. 2. (Color online) The calculated transmittance for the ZGNRs. The (a–g) labels refers to ribbons of Fig. 1. The red/solid and blue/dashed line refers to up and down spin, respectively.

ference of 1.2 eV is mainly due to the fact that the defect at the edge needs to move a small number of atoms than in the case (b) to obtain better formed pentagons. This is the same reason for the energy difference between (a) and (c) to be larger than between the (b) and (c) ribbons. Notice that the 5557777 defect in (d) and (e) ribbons, although in different positions with respect to the ribbon edge, have energies that differ by only 57 meV. The defect in these ribbons is extensive and two SW defects in the pentagon bonds make the carbon bonds to have similar lengths, without the larger bonds found in the structures (a) and (b). The deformation in those bonds localized far away from the defect area was small, causing leading to similar energies between (d) and (e) structures.

One important issue in the study of ZGNRs is their transport properties and the effect of defects. Therefore we performed transport calculations using the relaxed structures of Fig. 1 to obtain the transmittance curves showed in Fig. 2. The curves present a different behavior when compared to T of the case of a perfect ribbon (degenerate states with $0.5G_0$, per spin channel). The up and down transmittances (T_{up} and T_{down}) in all cases exhibited a decrease in magnitude and a strong spin anisotropy at the Fermi level. In most cases, a very large decrease in T_{down} was observed, except the cases (a) and (f) of Fig. 2. The high value of T observed in (a) indicates that ribbons with small deformations at the edge atom bonds had a similar behavior of a perfect ribbon. The T_{up} is very high in all cases except when the defect is at the edge, (f) and (g). On the other hand, ribbons with small deformation in the edge carbon atoms around the defects, (a), (c), and (d) cases, had a high T_{up} , almost constant in energy window of 0.2 eV around the Fermi level. The ribbons (b),

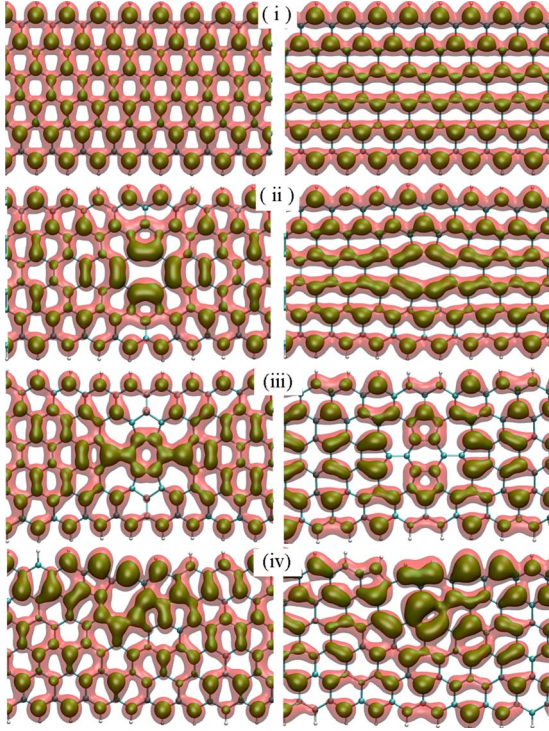


FIG. 3. (Color online) LDOS isosurfaces at the Fermi level. Left and right panels are display up and down channels, respectively. The red color refers to 0.0002 eV/Bohr (iso1) and the green color refers to 0.001 eV/Bohr (iso2). (i) perfect ribbon, (ii) 585 defect at the center, (iii) 55557777 longer defect at the center, and (iv) 585 defect at the edge.

(e), (f), and (g) presented broad dips around the Fermi level indicating a connection between this behavior and bond distortion of defect carbons at the edge.

The spin polarization at the Fermi energy can be measured by:²⁰

$$\xi = \frac{T_{\text{up}} - T_{\text{down}}}{T_{\text{up}} + T_{\text{down}}} \quad (1)$$

The values of ξ for each structure are given in Fig. 2. The polarization for the structures (b), (d), and (e) are very high, more than 90%, with a loss of transmittance close to 37%. The structure (g) presented a 75% polarization, with a moderate loss close to 50% in the up channel of the transmittance.

To help the understanding of the transport results of the ZGNRs we also calculated the LDOS at the Fermi level²⁶ using the:

$$\eta^{\sigma}(\vec{r}, E) = -\frac{1}{\pi} \lim_{\delta \rightarrow 0^+} \sum_{i,j} \text{Im}[G_{i,j}^{\sigma}(E + i\delta)] \phi_i(\vec{r}) \phi_j(\vec{r}), \quad (2)$$

where $\phi_i(\vec{r})$ are the orbitals used in *ab initio* calculations, the indices i and j denote all quantum indices of these orbitals, σ indicates the spin and $G_{i,j}^{\sigma}$ is the green function of scattering region.

Figure 3 presents LDOS isosurfaces of selected structures studied so far: (i) pure ribbon, (ii) ribbon (a), (iii) ribbon (d),

and (iv) ribbon (g). The analysis of the LDOS helps to understand two possible mechanisms of those responsible for the transport results. We found two mainly. First, we note in the ZGNRs with defects a reduction for spin down states in some regions of the ribbon or the complete absence of states in some carbon atoms, reducing the electron transmission throughout the ribbon. Second, the concentration of states in the defect atoms acts as a scattering center. The two isosurfaces depict states with values of 0.0002 eV/Bohr (iso1) and 0.010 eV/Bohr (iso2) delimiting a large spatial region with LDOS values.

In the pure ribbon of Fig. 3(i), we can see that the states are symmetrically distributed showing that there are no regions that difficult transmission or enhance scattering along the ribbon. The integration of the LDOS showed that half of all states are in the region delimited by iso1 and iso2. The other half are inside iso2 for both spin channels. In Fig. 3(ii), the down channel presented a similar behavior to the perfect ribbon, the up channel, on the other hand, displayed some concentration of states at the defect atoms acting as scattering centers and also a reduction of states at the edge atoms reduced the transmission. This provided an explanation for why the T_{up} value was lower than T_{down} in this case.

Ribbon (d) in Fig. 3(iii) was a very interesting case presenting the possibility for the defect to be metastable in the ribbon. When compared with the up states of pure ribbon we noted an enhancement of up states in the central region with a reduction in the edge states. The up channel showed states continuously distributed in the central region, enhancing transmission. This explains why T_{up} presented a high value (37% reduction in comparison with the pure ribbon), although there is a reduction of edge states. On the other hand the down channel showed a clustering of states in some atoms with spatial separation of isosurfaces of neighboring atoms, the reduction of states in the central region reduced transmission, giving a value of T_{down} close to zero. The metastable ZGNR presented a spin polarization of 94% being a very good candidate for spin filter due to its almost half metal behavior.

Ribbon (g) in Fig. 3(iv) had a large concentration of states in the atoms surrounding the defect, evidenced by the larger volume enclosed by their isosurfaces, making them scattering centers for the electrons. Although the up channel isosurfaces enclose a large spatial region connecting both leads, those states had a more disordered distribution when compared with the pure ribbon and presented high and low values at different atoms, causing a reduction around 50% of T_{up} due to scattering. The concentration of states on the defect atoms for the down channel was larger than those for the up states, indicating an enhancement of the scattering in these regions for T_{down} . The absence of down states in some atoms far from the defect reduced the transmission of electrons. These two factors reduced drastically the value of T_{down} justifying the transmittance results presented previously in Fig. 2.

In conclusion we have shown that the effect of defects in ZGNRs can be very dramatic, changing the transport behavior of the electrons from the spin degenerate case of pure ZGNR to highly spin polarized states, in some cases showing

more than 90% spin polarization, close the half metal behavior. These results were achieved by *ab initio* electronic structure calculations for ZGNRs with divacancy defects and by first principle transport calculations. We also presented electronic LDOS isosurface calculations that helped the understanding of the transport results. We think that, at the present time, it is possible to experimentally produce the structures studied here. Moreover, we strongly believe that this work can be useful to experimentalists as well as theo-

reticians to study GNRs, mainly in novel spintronics applications.

The authors acknowledge financial support from the Brazilian Funding Agencies CNPq, and, FAPESP and Capes. Thanks to CENAPAD-SP and IFGW-UNICAMP for use of the computational facilities. R.Y.O. thanks CAPES for a grant and E. P. M. Amorim, R. Faccio, and T. Martins for enlightening discussions regarding the present work.

-
- ¹W. Andreoni, *The Physics of Fullerenes Based and Fullerene Related Materials* (Springer, New York, 2000).
- ²R. Saito, G. Dresselhaus, and M.S. Dresselhaus, *Physical properties of carbon nanotubes* (Imperial College Press., London, 1998).
- ³K. S. Novoselov, A. K. Geim, S. V. Morozov, D. Jiang, M. I. Katsnelson, V. Grigoreva, and S. V. Dubonos, *Nature* (London) **438**, 197 (2005).
- ⁴Y. Zhang, Y.-W. Tan, H. L. Stormer, and P. Kim, *Nature* (London) **438**, 201 (2005).
- ⁵S. Stankovich, D. A. Dikin, G. H. B. Dommett, K. M. Kohlhaas, E. J. Zimney, E. A. Stach, R. D. Piner, S. T. Nguyen, and R. S. Ruoff, *Nature* (London) **442**, 282 (2006).
- ⁶H. C. Schniepp, J.-L. Li, M. J. McAllister, H. Sai, M. Herrera-Alonso, D. H. Adamson, R. K. Prudhomme, R. Car, D. A. Saviile, and I. A. Aksay, *J. Phys. Chem. B* **110**, 8535 (2006).
- ⁷A. H. Castro Neto, F. Guinea, and N. M. R. Peres, *Phys. World* **19**, 33 (2006).
- ⁸M. I. Katsnelson and K. S. Novoselov, *Solid State Commun.* **143**, 3 (2007).
- ⁹M. I. Katsnelson, K. S. Novoselov, and A. K. Geim, *Nat. Phys.* **2**, 620 (2006).
- ¹⁰Y. Kobayashi, K.-I. Fukui, T. Enoki, K. Kusakabe, and Y. Kaburagi, *Phys. Rev. B* **71**, 193406 (2005).
- ¹¹Y. Niimi, T. Matsui, H. Kambara, K. Tagami, M. Tsukada, and H. Furukawa, *Phys. Rev. B* **73**, 085421 (2006).
- ¹²M. Fujita, K. Wakabayashi, K. Nakada, and K. Kusakabe, *J. Phys. Soc. Jpn.* **65**, 1920 (1996).
- ¹³K. Nakada, M. Fujita, G. Dresselhaus, and M. S. Dresselhaus, *Phys. Rev. B* **54**, 17954 (1996).
- ¹⁴Y. Kobayashi, K.-I. Fukui, T. Enoki, and K. Kusakabe, *Phys. Rev. B* **73**, 125415 (2006).
- ¹⁵H. Lee, Y.-W. Son, N. Park, S. Han, and J. Yu, *Phys. Rev. B* **72**, 174431 (2005).
- ¹⁶Y. W. Son, M. L. Chen, and S. G. Louie, *Phys. Rev. Lett.* **97**, 216803 (2006).
- ¹⁷J. M. Carlsson and M. Scheffler, *Phys. Rev. Lett.* **96**, 046806 (2006).
- ¹⁸G.-D. Lee, C. Z. Wang, E. Yoon, N.-M. Hwang, and K. M. Ho, *Phys. Rev. B* **74**, 245411 (2006).
- ¹⁹R. G. Amorim, A. Fazzio, A. Antonelli, F. D. Novaes, and A. J. R. da Silva, *Nano Lett.* **7**, 2459 (2007).
- ²⁰T. B. Martins, R. H. Miwa, A. J. R. da Silva, and A. Fazzio, *Phys. Rev. Lett.* **98**, 196803 (2007).
- ²¹J. M. Soler, E. Artacho, J. D. Gale, A. García, J. Junquera, P. Ordejón, and D. Sánchez-Portal, *J. Phys.: Condens. Matter* **14**, 2745 (2002).
- ²²P. Hohenberg and W. Kohn, *Phys. Rev.* **136**, B864 (1964).
- ²³N. Troullier and J. L. Martins, *Phys. Rev. B* **43**, 1993 (1991).
- ²⁴J. P. Perdew, K. Burke, and M. Ernzerhof, *Phys. Rev. Lett.* **77**, 3865 (1996).
- ²⁵F. D. Novaes, A. J. R. da Silva, and A. Fazzio, *Braz. J. Phys.* **36**, 799 (2006).
- ²⁶Y. Xue, S. Datta, and M. A. Ratner, *Chem. Phys.* **281**, 151 (2002).
- ²⁷J. Heurich, J. C. Cuevas, W. Wenzel, and G. Schon, *Phys. Rev. Lett.* **88**, 256803 (2002).